Supporting Information

for

High-κ elastomer with dispersed ferroelectric nematic liquid crystal microdroplets

Fan Ye,[a] Chen Yang,[a] Xinxin Zhang,[a] Xiang Huang,[a] Yongmei Zhu,[a] Satoshi Aya[a,b], Mingjun Huang*[a,b]*

[a] South China Advanced Institute for Soft Matter Science and Technology, School of Emergent Soft Matter, South China University of Technology, Guangzhou 510640, China.

[b] Guangdong Provincial Key Laboratory of Functional and Intelligent Hybrid Materials and Devices, Guangdong Basic Research Center of Excellence for Energy & Information Polymer Materials, South China University of Technology, Guangzhou 510640, China;

Contents:

1. Materials and methods.

Materials. All commercial chemicals and solvents were used as received unless stated otherwise. All the commercial reagents were used without purification. p-toluenesulfonic acid (p-TsOH) was obtained from Acros. 4-dimethylaminopyridine (DMAP), and toluene were obtained from Sigma-Aldrich. Tetrahydrofuran (THF, Energy Chemical). Dichloromethane (DCM, Energy Chemical), Petroleum ether (PE, Energy Chemical) Ethyl acetate (EA, Energy Chemical), Methanol (MeOH, Energy Chemical, reagent grade). 2-Methyl-1,3-propanediol (95%, Bide), 2-Propylpropane-1,3-diol (95%, Bide), 3,5-Difluorobenzaldehyde (98%, Bide), 2,6-Di-tert-butyl-4-methylphenol (98%, Bide), n-Butyllithium (1.6mol/l in hexane, Energy Chemical), 2,6-Difluoro-4-bromobenzonitrile (98%, Energy Chemical), Bis(pinacolato)diboron (98%, Energy Chemical), 4-Bromo-3-(trifluoromethyl)phenol (98%, Energy Chemical), Potassium carbonate (K_2CO_3, 98%, Energy Chemical), N,N'-Dicyclohexylcarbodiimide (DCC, 98%, Energy Chemical), Tris(dibenzylideneacetone)dipalladium(0) (98%, Energy Chemical), 2,6-Difluoro-4-hydroxybenzonitrile (97%, Energy Chemical), Dicyclohexyl(2',6'-dimethoxy-[1,1'-biphenyl]-2-yl)phosphine (SPhos, 98%, Bide). The elastomer precursor, Sylgrad 184 PDMS silicone, was purchased from Dow Corning. Electroluminescent phosphor ZnS:Cu microparticles with an average diameter of 25 μm were purchased from Shanghai Keyan.

Reactions were carried out under a nitrogen atmosphere using a magnetic stirring hotplate and monitored by thin-layer chromatography (TLC) using an appropriate solvent system. Silica-coated aluminum TLC plates used were purchased from Merck (Kieselgel 60 F-254) and visualized using UV light at wavelengths of both 254 nm and/or 365 nm. Column chromatography was performed using the SepaBean™ Flash Chromatography System from Santai Technologies (40 - 63μm particle size).

Preparation of room-temperature stable N_F LC formula: The room-temperature stable N_F LC mixture was prepared by mixing the Y1, Y2, and Y3 at a 1:1:1 weight ratio, dissolving it into chloroform. After mechanical mixing and ultrasonic treatment, the solvent was mildly evaporated at 55 ℃. A uniform milky

liquid was obtained.

Preparation of FE composite samples: The N_F LC formula was weighted by mass fraction respectively and configured to the solutions of 10 mg μL^{-1} using ultradry THF solvent pre-filtered through a PVDF microporous membrane with 0.45 μm pore diameter. The PDMS precursor was prepared by mixing the base and crosslinker at a 10:1 weight ratio and then added into solutions with the N_F LC formula according to mass fraction respectively. After mechanical mixing and ultrasonic treatment, all mixtures were vacuumed to remove THF. Continue mechanical mixing to get uniform dispersion of FE composite precursors. Subsequently, the emulsion was degassed and poured into all kinds of mold. Curing at 60 °C for 1 h and 100 °C for 1 h yielded FE composite elastomers.

Density Functional Theory (DFT) Calculation: All DFT calculations were performed with the Gaussian 09 series of programs (Gaussian 09, Revision A.03). The DFT method of B3LYP/6-31g(d) basis set was used.

Nuclear Magnetic Resonance (NMR) Spectroscopy: ^{1}H, ^{19}F NMR spectra of the samples were obtained in $CDCl_3$ (Innochem, 99.8 atom % D, with 0.03%(v/v) TMS) solvents utilizing JASTEC JMTC-500/54/JJ 500 MHz NMR spectrometer. 1H NMR spectra were referenced to the residual proton impurities in $CDCl_3$ at δ 7.26 ppm)

Polarized Optical Microscopy (POM): The mixtures were introduced to homemade LC slabs with controlled thickness and alignment conditions. As planar alignment materials, we used KPI-3000 (Shenzhen Haihao Technology Co., Ltd). Homemade 5-μm-thick slabs with planar alignment were used for measuring polarized optical microscopy (POM, Olympus BX51) textures of the N_F LC formula. The temperature was controlled by the Instec mK2000 hot stage. The photographs of POM were taken with the camera (Nikon D5300). For measuring FE composites, the emulsions were spinning coating on a clean glass substrate, and curing as the same method mentioned above. The thickness of the film was around 30 μm. The input light is polarized and focused on the samples by a 50× objective.

Differential Scanning Calorimetry (DSC): The thermal properties of all the samples were characterized by utilizing a TA Instruments DSC 2500 with an

Intercooler 2P apparatus. The temperature and heat flow scales were calibrated at different heating and cooling rates (10 K min^{-1}) using a series of standard materials. For each run of the experiments, the initial mass of the samples used was about 10 mg under nitrogen flow

Thermogravimetric Analysis (TGA): The isothermal decomposition experiments were carried out in a thermogravimetric analysis instrument (Model Q500, TA Instruments) protected with nitrogen atmosphere. For each run of the experiments, the initial mass of the samples used was about 5 mg, scanned within the temperature range of 30 °C to 500°C with a heating rate of 10 °C/min.

Mechanical Measurements: The FE composite samples were cured in a dumbbell-shaped PTFE mold with dimensions of 12 mm×2 mm×1 mm. Tensile tests were performed by using the Electronic Testing Machine (LD22.102, LiShi, Shanghai). All tensile tests were performed at a constant strain rate of 20 mm min^{-1} with a 100 N load cell under ambient conditions (20 °C, RH 40%). The tensile tests adopted the single axial tension mode.

Dielectric spectroscopy: Dielectric spectroscopy was conducted by using an LCR meter (E4980A, Keysight). The data collection of the frequency and temperature sweeping are automated by homemade software written in Labview. Homemade 20-μm-thick ITO-coated slabs without parallel alignment layers were used for measurements of the N_F LC formula. The voltage applied to the ITO cell is 50 mV_{rms}. For dielectric measurements of FE composites, the degassed emulsions were spin-coated on clean ITO glass and sandwiched by another ITO glass. The thickness of the cell was controlled via a very small amount of polystyrene spacers (particle size: 30 μm, Suzhou Knowledge & Benefit Sphere Tech. Co., Ltd.) located at the four corners. After curing completely, the applied voltage is 1 V_{rms}. The scanning frequency was from 20 Hz to 1 MHz, and the temperature range was from 25 to 110 °C. Then the corresponding effective dielectric constant was back-calculated.

Polarization-Electric field (P-E) Loops Measurements: The polarization switching measurements were conducted using the ferroelectricity measurement system (TOYO FCE10-S, Japan) combined with a waveform generator (Tabor Electronic,

WW5064), high-voltage linear amplifier (pendulum, A800), and analyzer (TOYO, Model 6252). The samples used were the same as those of dielectric measurements. The electric fields were from 10 kV cm^{-1} to 80 kV cm^{-1}, and the temperature range was from 25 to 110 °C.

Dielectric Breakdown Strength: The dielectric breakdown strength was measured using a high voltage breakdown tester (BDJC-50KV) at room temperature. The testing samples were soaked in silicone oil. DC Voltage rise rate was set as 500 V s^{-1}, and 15 data were obtained for each sample and analyzed by the two-parameter Weibull statistic. The sample was prepared by blade coating on a clean glass and then cured as mentioned before. The resulting film was sputtered gold electrode and then cut into 14 mm diameter slices for test.

ACEL Device. The ACEL layer was prepared by grinding 50 wt% EL phosphor microparticles in the N_F LC-containing elastomer precursor, followed by blade coating to form samples with a thickness of 50 μm. The EL layer was sandwiched between two transparent ITO glasses. AC voltage signals (standard sine wave) to achieve the ACEL devices were generated by a function/arbitrary waveform generator (DG4102, RIGOL) and amplified by a high-voltage power amplifier (HA-405, PINTECH). The luminance values were measured by a luminance meter (TES 137, TES Electrical Electronic).

Synthesis of liquid crystal molecules. The detailed synthesis methods of liquid crystal molecules have been reported in the references S2, and S3.[S2,S3]

2. Additional POM images for N_F LC formula after 2 months.

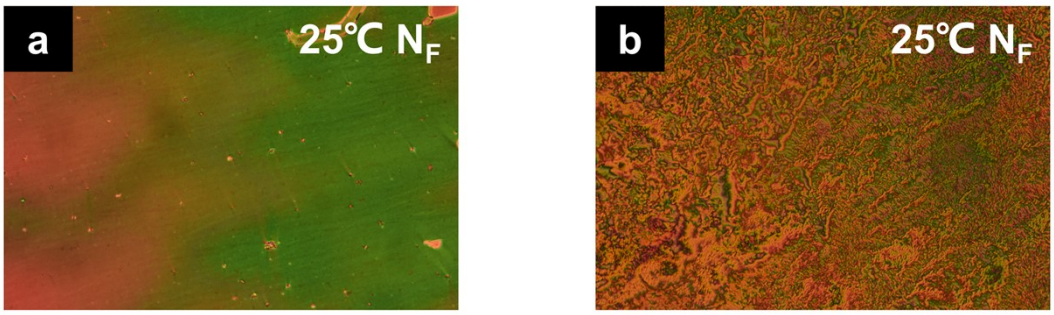

Figure S1. Room-temperature stability test of N_F LC formula in the NF Phase. (a) POM image (×10) of freshly prepared sample in a parallel rubbing alignment cell. (b) POM

image (×10) of N_F LC formula in the same cell after 2 months. Cell thickness: 10 μm.

3. 3D dielectric plots and P-E loops of N_F LC formula.

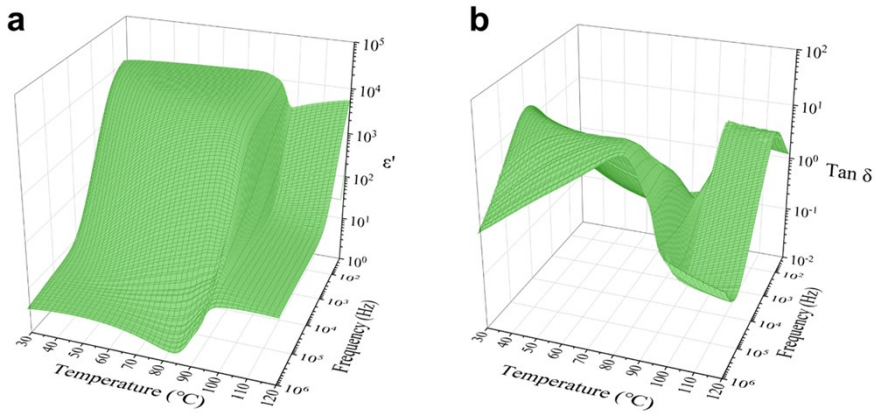

Figure S2. Three-dimensional plots of the real (a) and imaginary (b) components of the complex permittivity versus temperature and frequency.

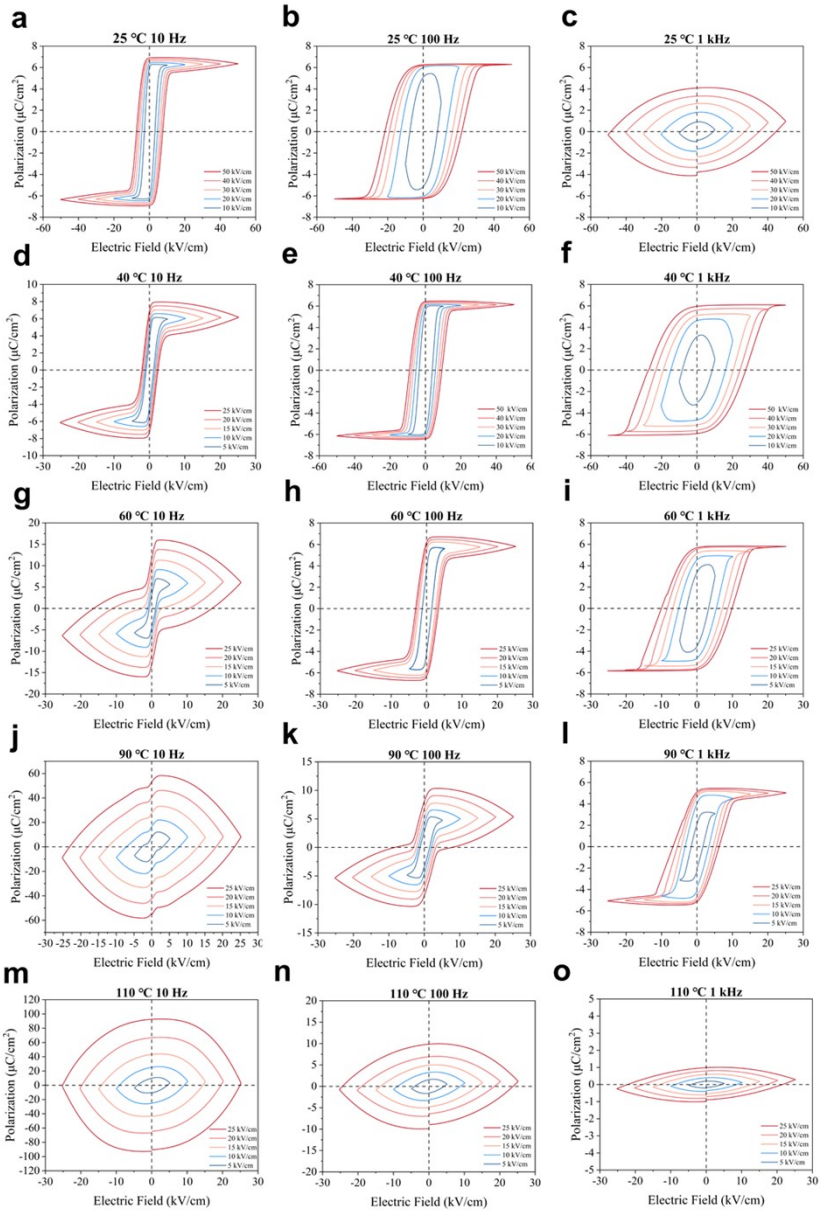

Figure S3. P-E hysteresis loops of N_F LC formula at different temperatures (from up to down: 25 ℃, 40 ℃, 60 ℃, 90 ℃, 110 ℃). The poling frequency varies from left to right: 10 Hz, 100 Hz, 1000 Hz with a triangle wave function.

4. Morphology of FE composites in macro- and micro-exhibitions.

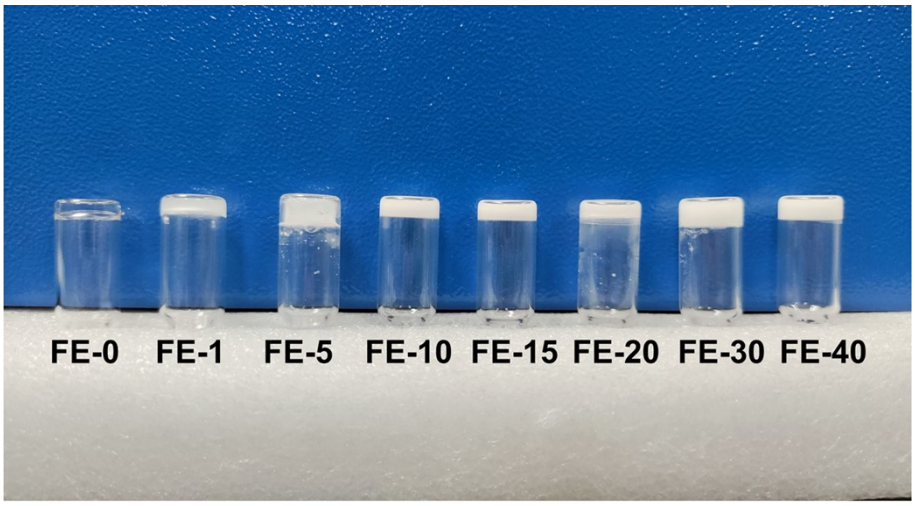

Figure S4. Morphology of composite elastomers with different LC concentrations. As the weight percentage of N_F LCs increases, haze becomes evident gradually.

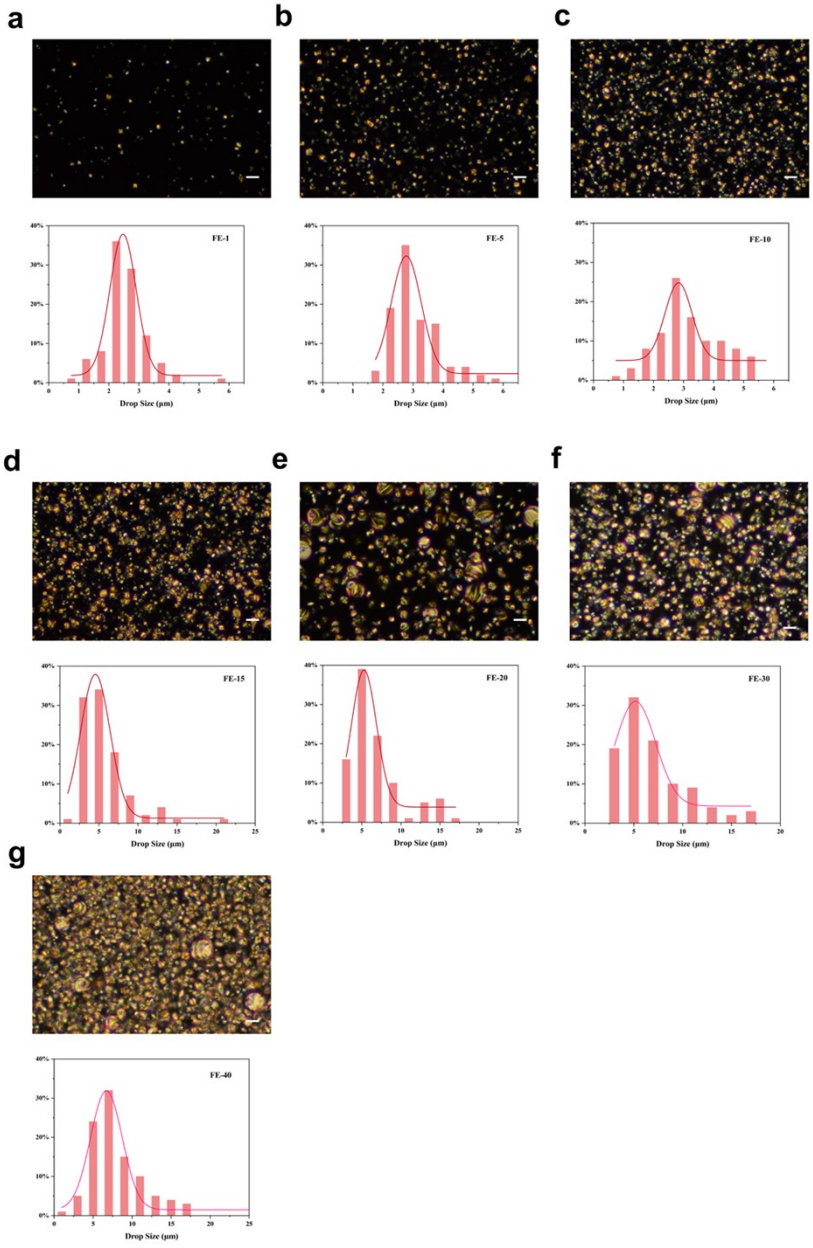

Figure S5. Morphology of N_F LC composite elastomers. POM images (up) under crossed polarizer, and histogram of the percent of analyzed droplets versus major radii (down). (a-g) Elastomers with different N_F LC concentration: 1wt%, 5 wt%, 10 wt%, 15wt%, 20 wt%, 30 wt%, 40 wt%. Scale bar: 10 μm.

5. Mechanical and thermal properties of FE composites.

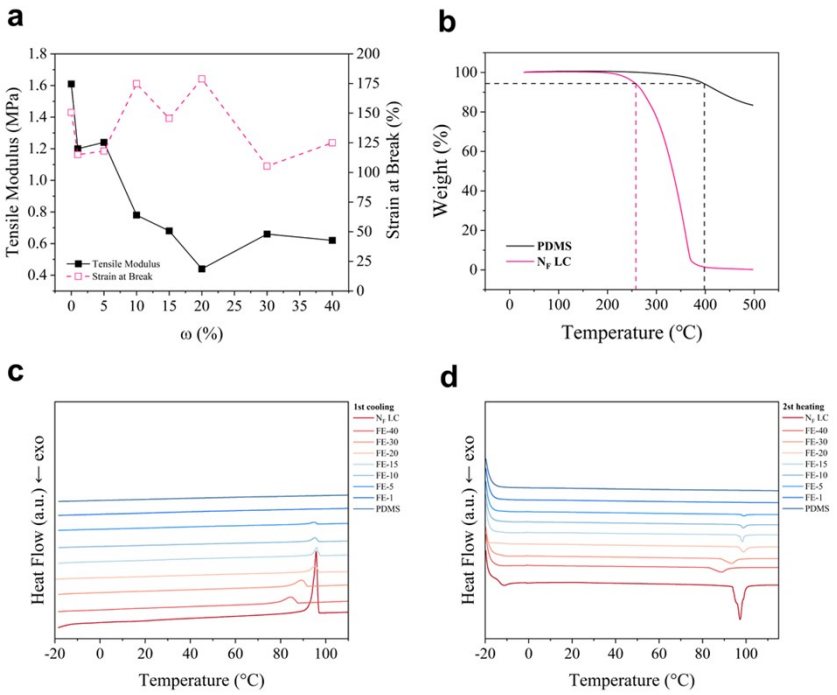

Figure S6. DSC curves of N_F LC composite elastomers. (a) First cooling curves. (b) Second heating curves. (c) TGA curves for pristine PDMS and N_F LC formula. The dash lines correspond to the temperature of 5 % thermal weight loss.

6. Dielectric frequency spectrum of FE composites in various temperatures.

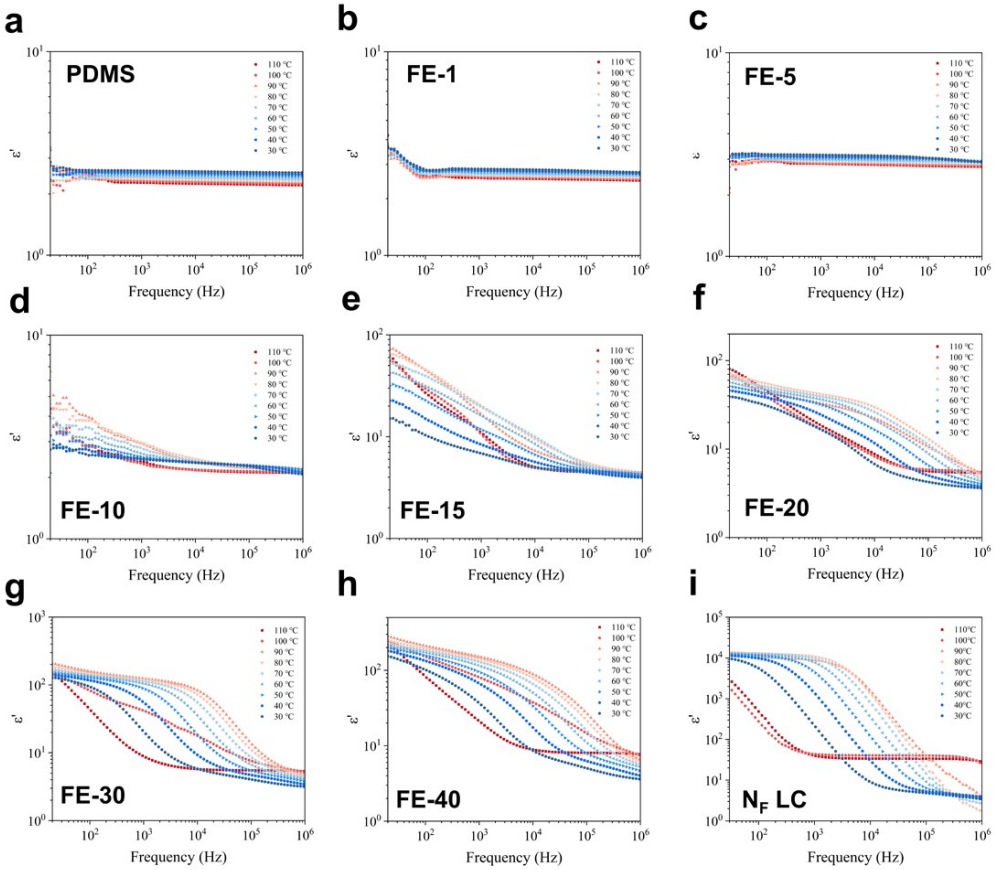

Figure S7. Frequency spectra of the real part of complex dielectric permittivity at different temperatures for (a) pristine PDMS, (b-h) composite elastomers with different N_F LC contents, and (i) N_F LC formula mixture.

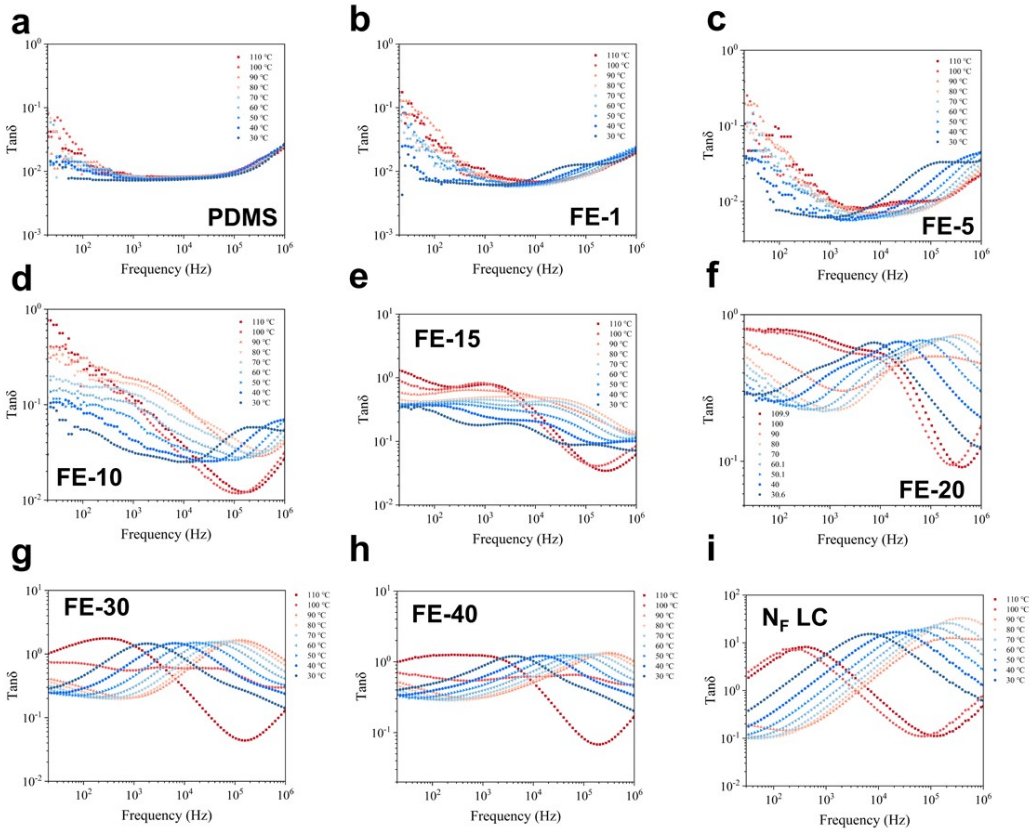

Figure S8. Frequency spectra of the dielectric dissipation loss at different temperatures for (a) pristine PDMS, (b-h) composite elastomers with different N_F LC contents, and (i) N_F LC formula mixture.

7. P-E loops of FE composites in various temperatures.

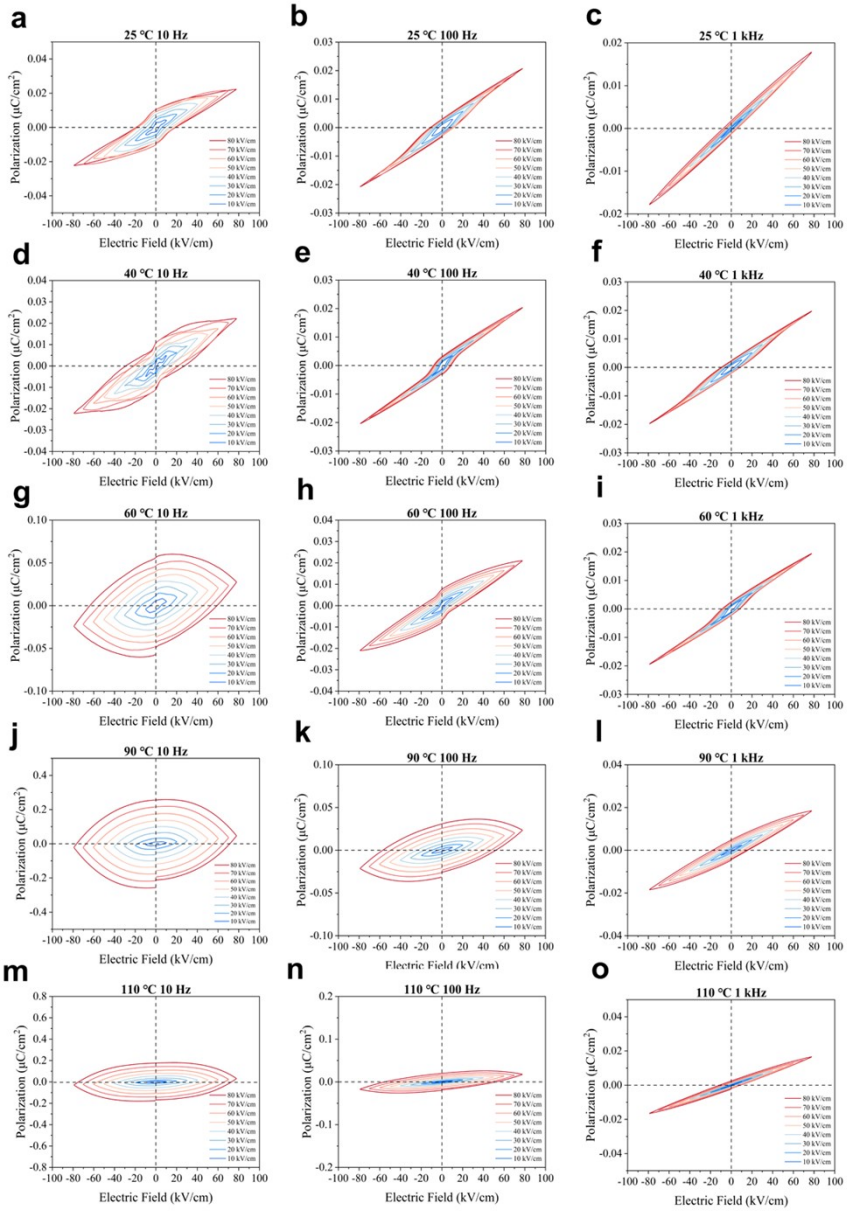

Figure S9. P-E hysteresis loops of FE-10 at different temperatures (from up to down: 25 ℃, 40 ℃, 60 ℃, 90 ℃, 110 ℃). The poling frequency varies from left to right: 10 Hz, 100 Hz, 1000 Hz with a triangle wave function.

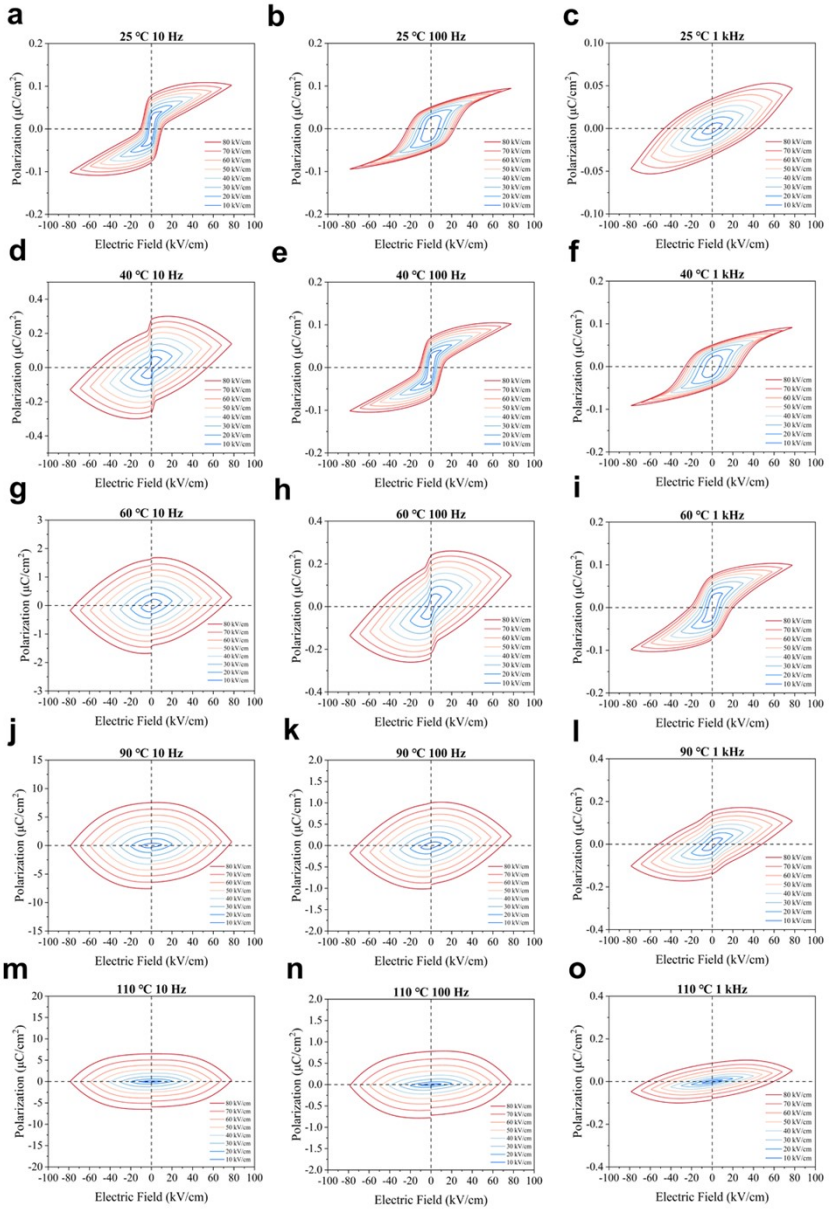

Figure S10. P-E hysteresis loops of FE-15 at different temperatures (from up to down: 25 ℃, 40 ℃, 60 ℃, 90 ℃, 110 ℃). The poling frequency varies from left to right: 10 Hz, 100 Hz, 1000 Hz with a triangle wave function.

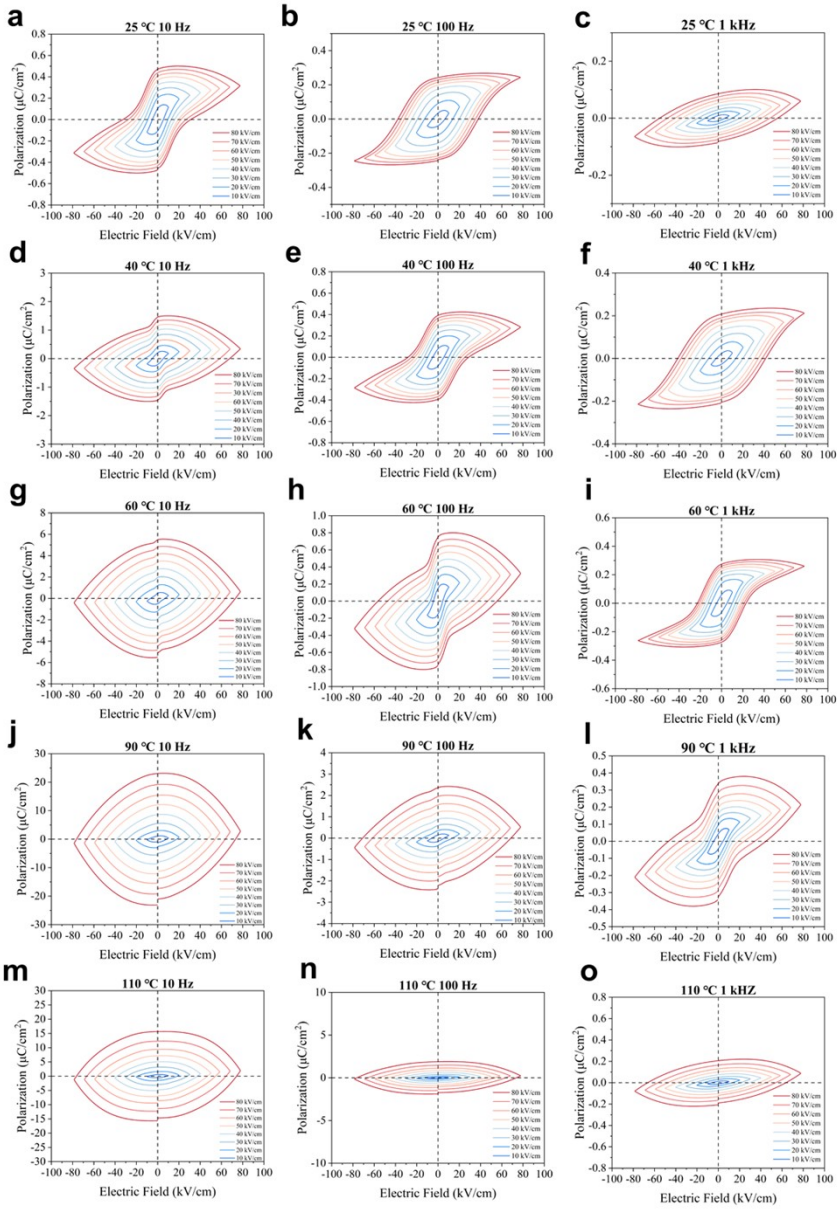

Figure S11. P-E hysteresis loops of FE-20 at different temperatures (from up to down: 25 ℃, 40 ℃, 60 ℃, 90 ℃, 110 ℃). The poling frequency varies from left to right: 10 Hz, 100 Hz, 1000 Hz with a triangle wave function.

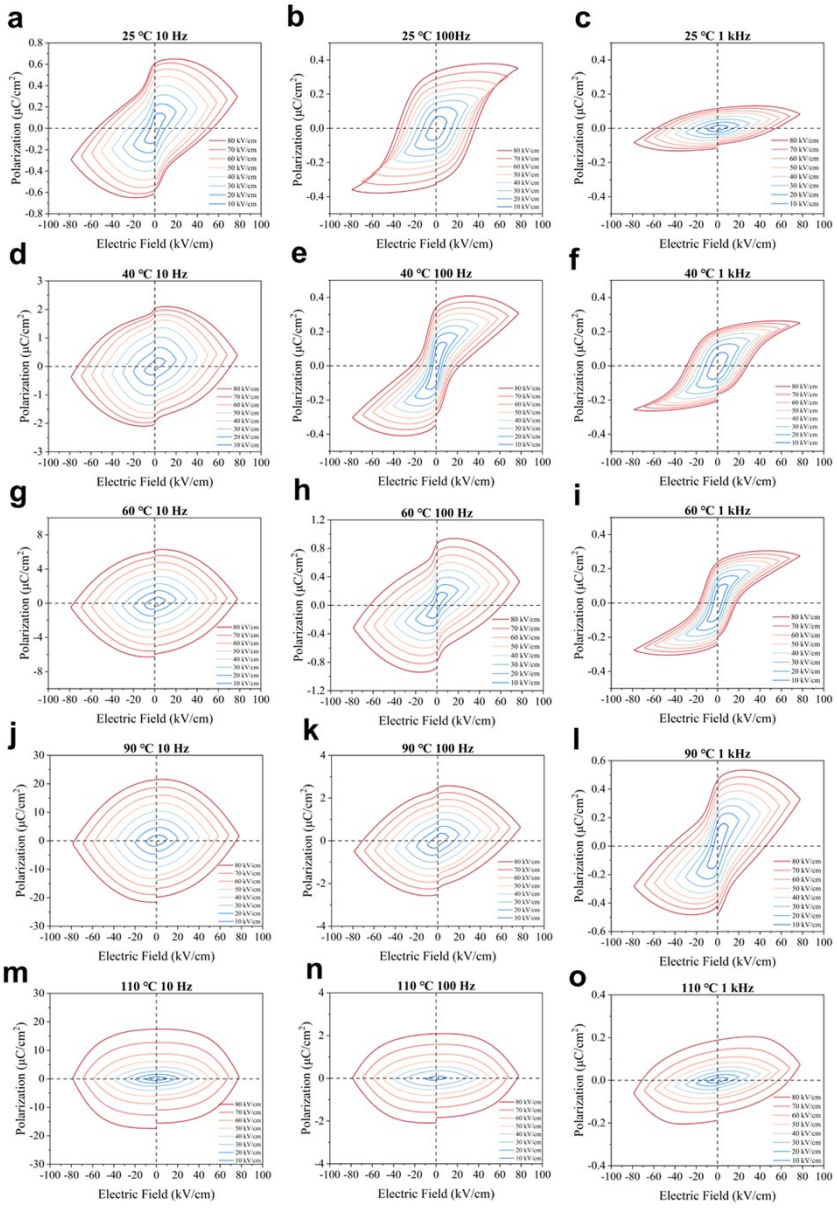

Figure S12. P-E hysteresis loops of FE-30 at different temperatures (from up to down: 25 ℃, 40 ℃, 60 ℃, 90 ℃, 110 ℃). The poling frequency varies from left to right: 10 Hz, 100 Hz, 1000 Hz with a triangle wave function.

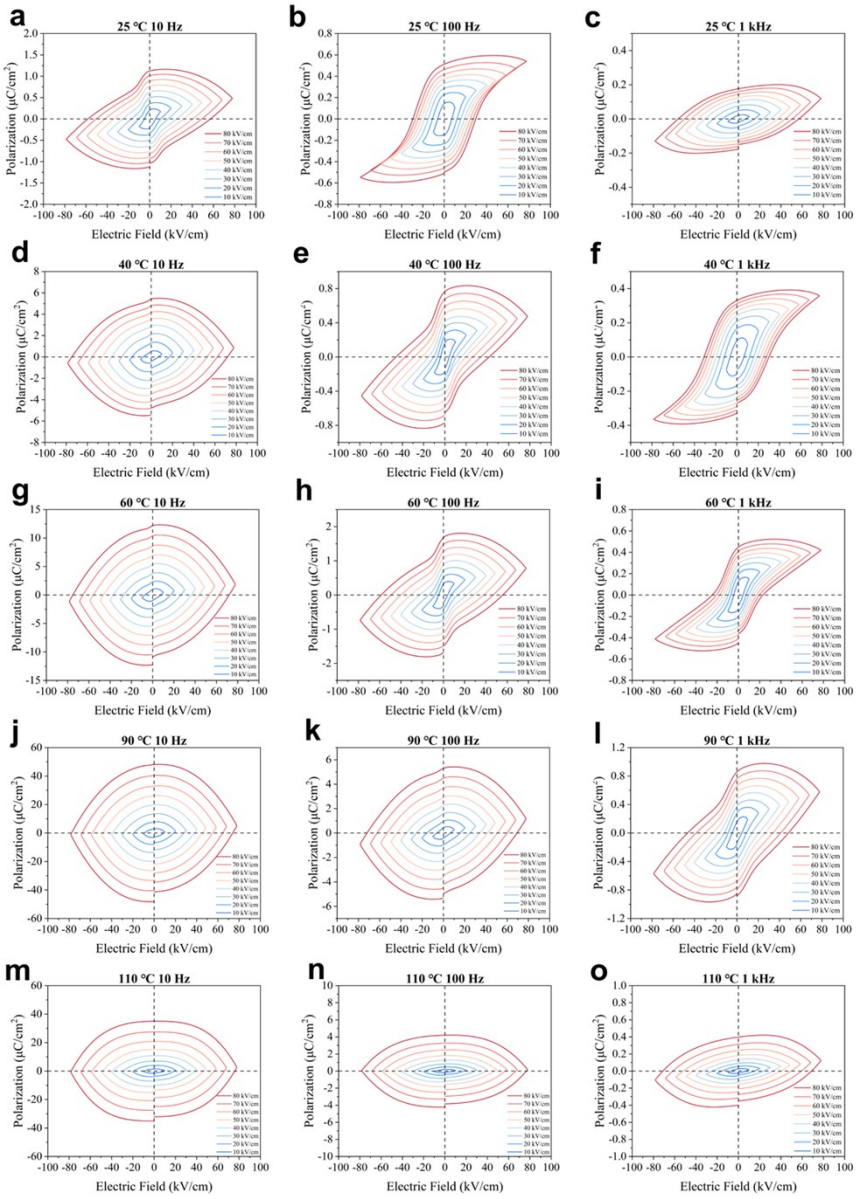

Figure S13. P-E hysteresis loops of FE-40 at different temperatures (from up to down: 25 ℃, 40 ℃, 60 ℃, 90 ℃, 110 ℃). The poling frequency varies from left to right: 10 Hz, 100 Hz, 1000 Hz with a triangle wave function.

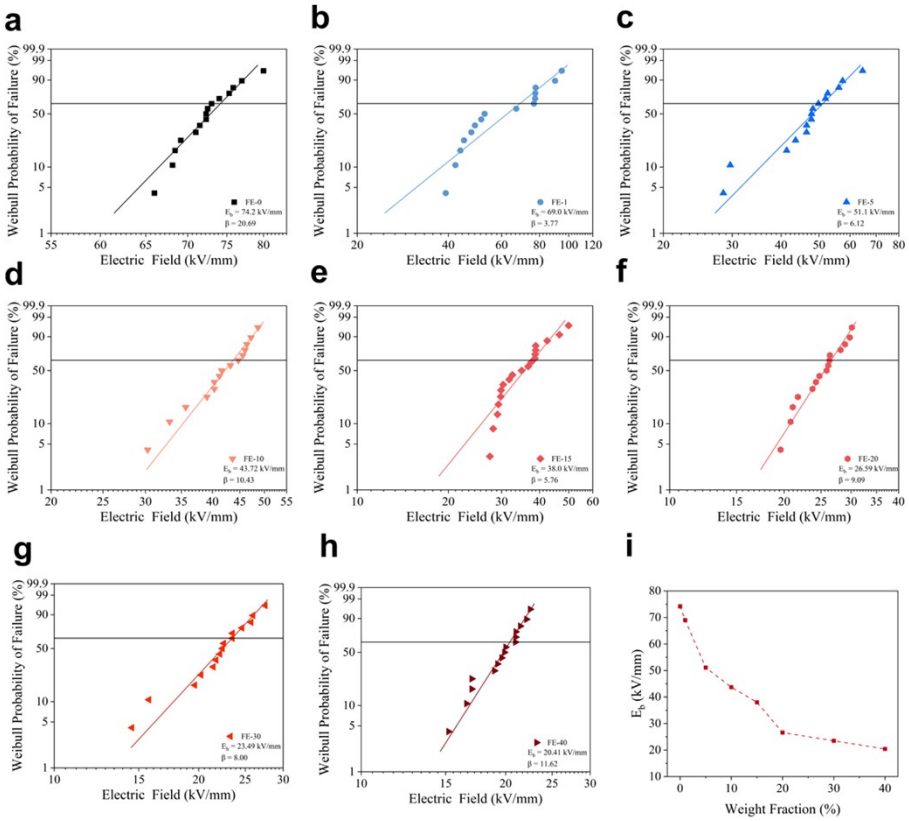

Figure S14. (a-h) Weibull breakdown strength of FE composites. (i) Weibull breakdown strength versus N_F LC weight fraction.

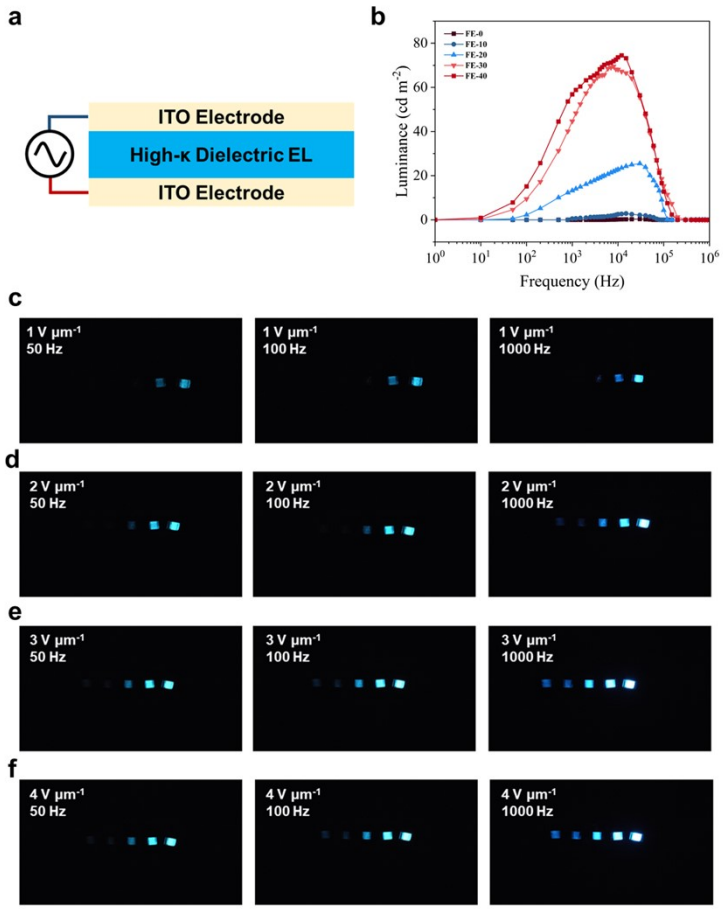

Figure S15. (a) Schematic diagram of AC based on FE composites. (b) Electroluminescence intensity versus frequency of applied field (4 V μm^{-1}). (c-f) Illustration of ACEL devices using different FE composites. In each photograph, from left to right: FE-0, FE-10, FE-20, FE-30, FE-40.

8. Reference

[S1]L. Shi, T. Zhu, G. Gao, X. Zhang, W. Wei, W. Liu, S. Ding, *Nat Commun* **2018**, *9*, 2630.

[S2]J. Li, H. Nishikawa, J. Kougo, J. Zhou, S. Dai, W. Tang, X. Zhao, Y. Hisai, M. Huang, S. Aya, *Science Advances* **2021**, *7*, eabf5047.

[S3]J. Li, Z. Wang, M. Deng, Y. Zhu, X. Zhang, R. Xia, Y. Song, Y. Hisai, S. Aya, M. Huang, *Giant* **2022**, *11*, 100109.